Journal of ELECTRONIC MATERIALS, Vol. 44, No. 1, 2015
DOI: 10.1007/s11664-014-3460-3

Effects of Cu, Zn on the Wettability and Shear Mechanical Properties of Sn-Bi-Based Lead-Free Solders

JUN SHEN[1,2,3], YAYUN PU,[1] HENGGANG YIN,[1] and QIN TANG[1]

1.—College of Materials Science and Engineering, Chongqing University, Chongqing 400044, China. 2.—e-mail: shenjun2626@163.com. 3.—e-mail: shenjun@cqu.edu.cn

Effects of minor Cu, Zn additions on the wettability, microstructures, and shear properties of Sn-Bi-based lead-free solder joints were investigated. The results show that a Cu addition promotes the wetting ratio of solder alloy, while Zn creates the opposite effect. The Cu_5Zn_8 intermetallic compound layer at the interface of Sn-40Bi-2Zn-0.1Cu and the Cu substrate alters the surface tension, which increases the contact angle. Also, this type of intermetallic compound contributes to the change of three wetting indicators. A proper amount of Cu, Zn increased the wetting force and decreased the wetting time, while the variation in the trend of withdrawing force is consistent with that of contact angle. From joint shear test results, the shear force decreased in the following order: Sn-40Bi-0.1Cu, Sn-58Bi, and Sn-40Bi-2Zn-0.1Cu solder joints. Cu additions refined the grain size of the Bi-rich phase and decreased the interface brittleness, which is the reason for the improvement of the shear strength of Sn-40Bi-0.1Cu solder joints. In contrast, Zn weakened the shear strength due to the brittle nature of the Zn-rich phase and the chemical activity of Zn.

Key words: Sn-Bi-based alloy, composite, wettability, shear property

INTRODUCTION

Because of the harmful influence of lead and lead-containing alloys on the environment and alpha radiation from impurities in Pb, a number of available Pb-free solder alloys (e.g., Sn-Bi, Sn-Ag, and Sn-Zn) are considered as potential lead-free alternatives to the classical Sn-Pb alloy.[1] Compared with traditional Sn-Pb alloy, Sn-Bi solders exhibit several intriguing characteristics such as low melting temperature and satisfactory wettability, being currently chosen for electronic packaging applications. Moreover, additional reasons for the popularity of Sn-Bi solder in low-cost electronic consumer products include its favorable properties of high tensile strength, creep resistance, and thermal fatigue.[2] However, it is well known that binary Sn-Bi alloy is primarily composed of a Sn-rich dendritic matrix and brittle Bi-rich phase, which leads to deterioration of mechanical properties. Furthermore, the wetting property between the solder and substrate is crucial to the reliability of soldered joints.[3]

In fact, several related studies have been performed, focusing on various Sn-Bi-based solders.[4,5] For the mechanical properties, Song et al.[6] revealed that the Bi-rich precipitates appearing in high-Bi samples lead to quick crack propagation. Adding exotic elements to refine the grain size is viewed as an advisable method to enhance the mechanical properties of Sn-Bi solder; For example, Yang et al.[7] reported that the microstructure of Sn-Bi composite solder can be refined by increasing alloying with graphite. Zhang and Chen suggested that addition of multiwalled carbon nanotubes could refine the grains and reduce the Bi content in the deposited Sn-Bi alloy.[8] Moreover, several beneficial effects of Zn or Cu addition on Pb-free solders have also been reported.[4,9] Zn addition promoted the mechanical properties of the solder and suppressed the growth of Cu_6Sn_5 IMC at the interface between the solder and the Cu substrate. Meanwhile, Cu-containing solders have lower corrosion resistance and higher mechanical strength. Therefore, the alloying method has been adopted for modifying solder properties.

(Received April 1, 2014; accepted October 6, 2014; published online November 1, 2014)

Since the wetting process plays an important role in soldering, the effect of Cu and Zn addition on the wettability and shear strength of Sn-Bi solders has been explored.

This study attempts to investigate the wettability, microstructures, and shear strength of solder joints made with newly developed Sn-40Bi-0.1Cu and Sn-40Bi-2Zn-0.1Cu alloys.

EXPERIMENTAL PROCEDURES

Specimen Preparation

Pure tin (99.999%), bismuth (99.999%), copper (99.999%), zinc (99.999%), and lead (99.999%) were used as raw materials. After weighing the individual pure metals, they were mixed and melted in a vacuum arc furnace under high-purity argon atmosphere. The molten solder (at 553 K) in the crucible was chill-cast in steel molds to form cylindrical ingots (Sn-58Bi, Sn-40Bi-0.1Cu, Sn-40Bi-2Zn-0.1Cu, and Sn-37Pb) with 30 mm diameter and 230 mm length and to form another group of cylindrical ingots of 60 mm diameter and 60 mm length. To obtain a homogeneous composition, all ingots were remelted five times.

Spreading Test

The experimental substrates were 99.99% purity oxygen-free copper plate with 30 mm length, 30 mm width, and 3 mm thickness. They were polished with diamond powders and cleaned in acetone, then degreased in 5% vitriol solution at 338 K for 1 min to remove surface oxides and impurities. Five pieces of specimens of Sn-58Bi, Sn-40Bi-0.1Cu, and Sn-40Bi-2Zn-0.1Cu solder alloys with 6.5 mm diameter and 1.24 mm length were machined from the cast ingots. Prepared lead-free solders were placed on plates to be manually soldered at temperature of 473 K for about 30 s. After soldering, the solder specimens were measured by a micrometer.

Wetting Balance Measurements

The surface tension of the copper substrates was measured using a wetting balance in accordance with JIS Z 3198 standard. Prepared oxygen-free copper substrates were mechanically cut into five slices with 0.3 ± 0.01 mm thickness, 10 ± 0.01 mm width, and 30 ± 0.01 mm length. Acetone was used to eliminate surface defects such as oil and blots, followed by washing in distilled water and ethanol. The alloys (Sn-58Bi, Sn-40Bi-0.1Cu, Sn-40Bi-2Zn-0.1Cu, and Sn-37Pb) were heated in a crucible with Rosin mildly activated (RMA)-type flux (JIS-K-5902) at 523 K to achieve the set temperature. Moreover, an extra group of Sn-40Bi-2Zn-0.1Cu solder with R04 flux was added for comparison, as this flux was effective in enhancing the wettability of Sn-40Bi-2Zn-0.1Cu on the Cu substrate. During the test, the ingot was placed in a crucible to maintain the axial symmetry of the liquid metal

Table I. Parameters of wetting balance measurements

Immersion into Flux		Immersion into Molten Solder Alloy				
Time (s)	Rising Velocity (mm/s)	Temperature (K)	Immersion Velocity (mm/s)	Rising Velocity (mm/s)	Hold Time (s)	Immersion Depth (mm)
5	10	523	5	5	10	2

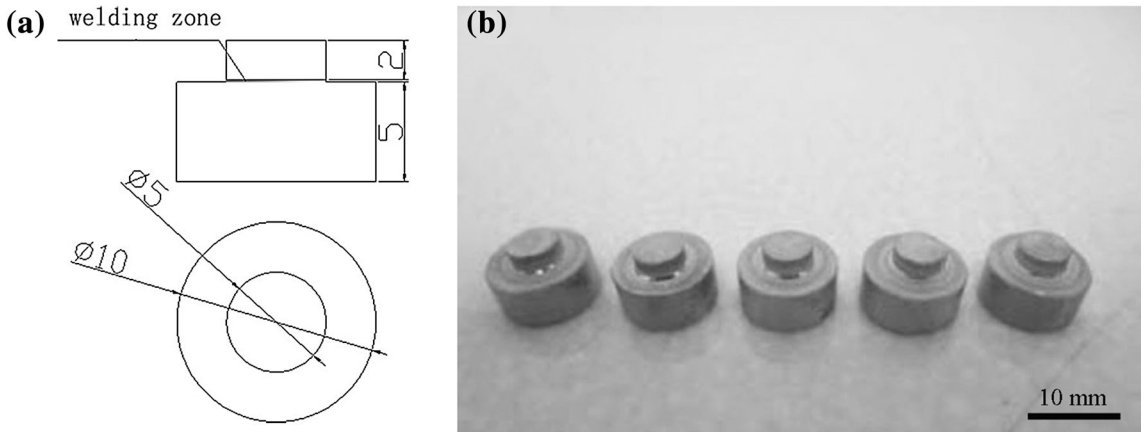

Fig. 1. (a) Dimension and (b) appearance of Sn-Bi-based/Cu solder joints for shearing strength tests.

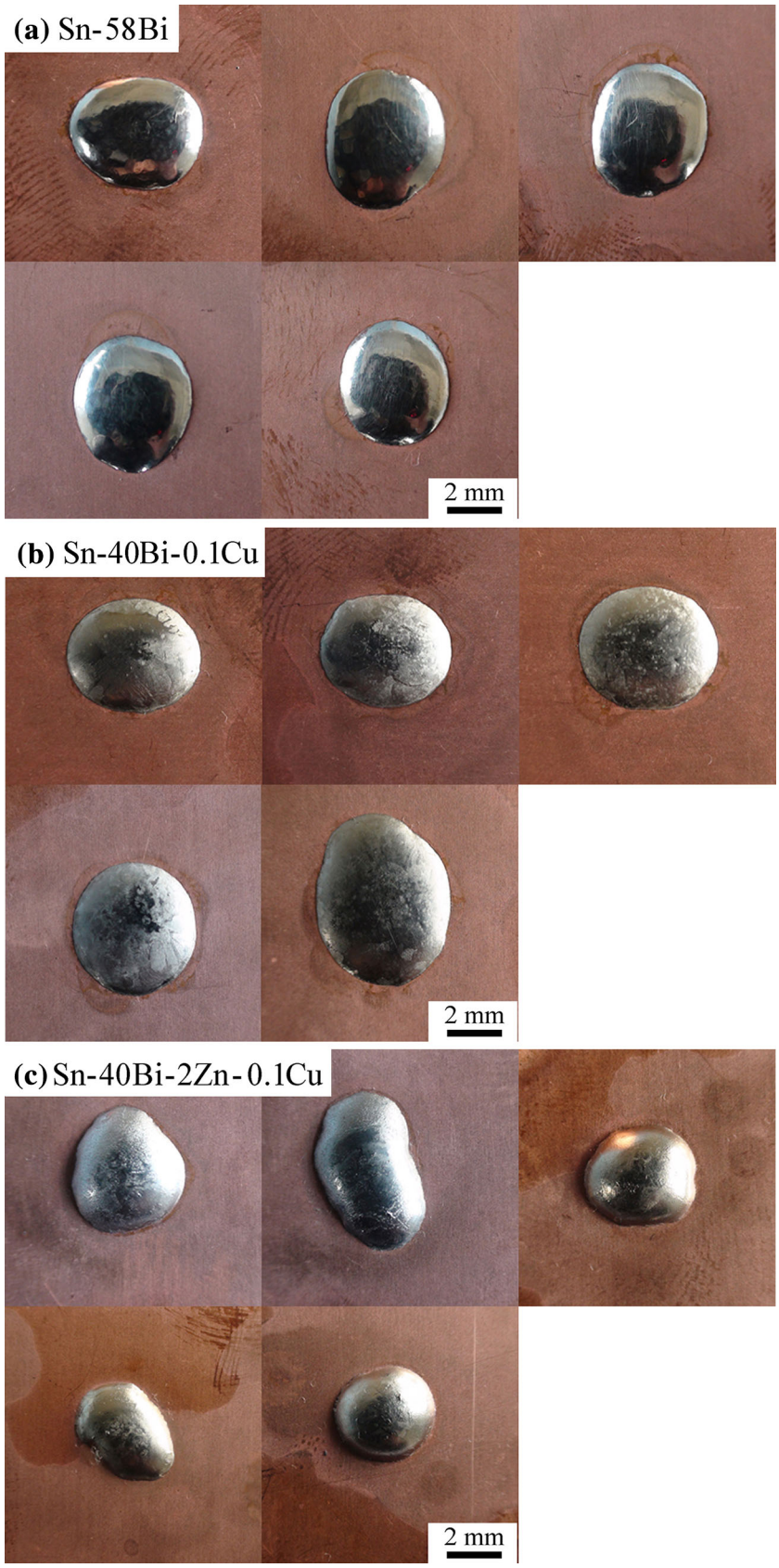

Fig. 2. Top-view optical images of Sn-Bi-based solder alloys spreading on Cu substrates: (a) Sn-58Bi, (b) Sn-40Bi-0.1Cu, and (c) Sn-40Bi-2Zn-0.1Cu.

Table II. Wettability for Sn-58Bi, Sn-40Bi-0.1Cu, and Sn-40Bi-2Zn-0.1Cu alloys

Alloy	Mass (g)	Height of Joint (mm)	Wetting Ratio (%)	Wetting Angle
Sn-58Bi	0.300 ± 0.007	1.11 ± 0.02	72.70 ± 0.52	29.7 ± 0.68
Sn-40Bi-0.1Cu	0.300 ± 0.004	1.08 ± 0.01	73.93 ± 0.20	25.5 ± 0.51
Sn-40Bi-2Zn-0.1Cu	0.300 ± 0.001	1.45 ± 0.04	64.88 ± 1.02	48.4 ± 1.76

drop. Prior to the test, a fixed amount of flux was applied onto the four copper substrates. Then, the substrate was dipped in liquid for 10 s. Table I presents the parameters used during the wetting balance measurements.

Shear Testing

Figure 1 shows the shape of the specimens used in the shear test. For each alloy composition (Sn-58Bi, Sn-40Bi-0.1Cu, and Sn-40Bi-2Zn-0.1Cu), the diameters of the soldered specimens were 5 mm and 10 mm and their lengths were 2 mm and 5 mm, respectively. A shear testing machine (Instron 5564) with 1 mm/min shear speed was used to investigate the shear properties of these alloys. The average strength of five samples was taken for each prepared solder. After shear testing, the fracture surfaces and compositions were thoroughly investigated by scanning electron microscopy (SEM, VegaII LMU; TESCAN, Inc.) equipped with an energy-dispersive x-ray (EDX) analyzer (ISIS300; Oxford, Inc.).

RESULTS AND DISCUSSION

Wetting Ratio and Contact Angle

Figure 2 presents top-view optical images of Sn-Bi-based alloy sessile droplets on pure copper, taken after quenching from the preset solder. The spreading of the molten solders on the pure Cu substrates occurred uniformly in the radial directions. Compared with Sn-58Bi, the surface glossiness of the Sn-40Bi-0.1Cu and Sn-40Bi-2Zn-0.1Cu solder alloys was more grey, especially for the latter. Moreover, with Zn addition, a significant increase in solder height was achieved. The equilibrium contact spreading ratio of solder on the Cu substrate is defined by the equation

$$S = \frac{D - H}{D} \times 100\%, \tag{1}$$

where S represents the spreading ratio, D is the diameter of the molten solder ball, and H is the height of the molten solder. Table II presents the calculated results for the wettability for the Sn-58Bi, Sn-40Bi-0.1Cu, and Sn-40Bi-2Zn-0.1Cu alloys. Obviously, the spreading ratio of Sn-40Bi-0.1Cu is the best whereas Sn-40Bi-2Zn-0.1Cu shows inferior wettability.

In the spreading test, the wetting angle was measured to evaluate the wettability for the molten solder. As shown in Table II and Fig. 3, the wetting angle of Sn-40Bi-0.1Cu decreased from 29.7° to 25.5° with minor Cu addition, while the wetting angle increased dramatically (48.4°) after Zn was added. Since the IMCs formed at the interface of the solder/Cu couple in a few seconds when the molten solder began to spread, the equilibrium contact angle determined by the interfacial surface tension can be represented as follows:[10]

$$\cos\theta = \frac{\gamma_{\text{s-air}} - \gamma_{\text{ls}}}{\gamma_{\text{l-air}}}, \tag{2}$$

where $\gamma_{\text{s-air}}$, γ_{ls}, and $\gamma_{\text{l-air}}$ represent the surface tensions of the substrate/air, liquid solder/IMC, and liquid/air interfaces, respectively. According to this equation, a small wetting angle requires a large ($\gamma_{\text{s-air}} - \gamma_{\text{ls}}$) or a small $\gamma_{\text{l-air}}$ value. In this study, although a certain amount of Zn atoms could be stored in the form of Cu-Zn IMC within the Sn-40Bi-2Zn-0.1Cu solder matrix, redundant Zn atoms still existed in free state when 0.1 wt.% Cu and 2 wt.% Zn were added (with the Cu content in Cu_5Zn_8 varying from 30% to 55%[11]). As reported, Zn is quite active and can be easily oxidized. These free Zn atoms caused a continuous oxidation film during the spreading process: atmospheric oxygen molecules could be absorbed by Zn atoms on the surface of the molten solder, and then capture electrons to form a ZnO film. This process provides a path for other oxygen molecules to pass through this oxide film and promotes diffusion reaction to form a thick oxide layer on the solder surface.[12] Hence, a higher $\gamma_{\text{l-air}}$ value was achieved and the expansion of the molten solder was prevented. In addition, the final contact angle not only is related to the surface tension of the liquid but also depends on the solid–liquid interfacial reaction. From the perspective of γ_{ls}, a larger value will lead to a larger value of θ. The IMCs formed at the interface can be changed by the addition of Zn, that further changing the γ_{ls}. As mentioned above, the formation of Cu-Zn IMC was greater than that of Cu-Sn IMC (as confirmed by Fig. 7). The first IMC phase generated at the metastable equilibrium state can be identified as the one with the largest driving force for formation. Indeed, the driving force of Cu-Zn IMC, which is equal to the Gibbs energy change per unit area released by the interfacial reaction, is greater than that of Cu-Sn IMC. Therefore, γ_{ls} became larger with the addition of Zn, which resulted in the larger θ.

Also, R04 flux was used to determine the effect of oxidation of Zn. Suitable fluxes form a continuous

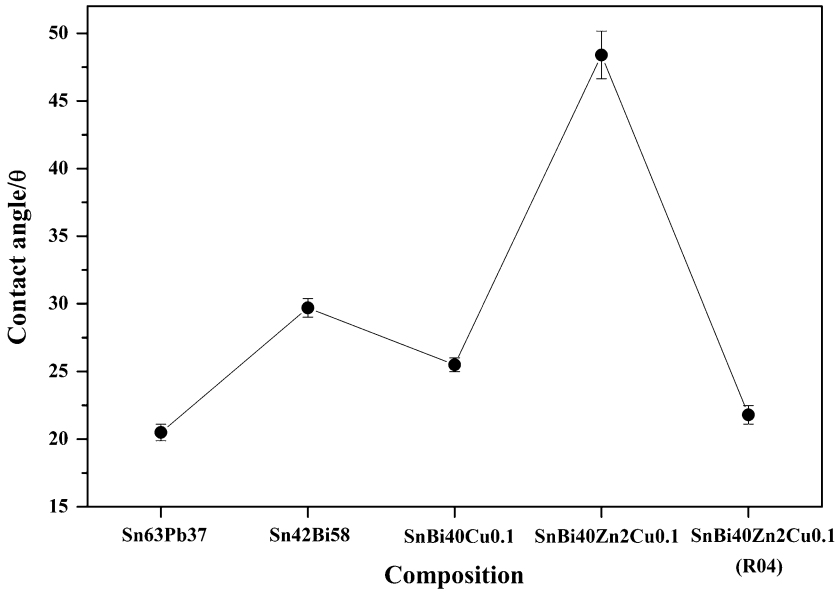

Fig. 3. Variation of contact angle for different solder alloys.

film over the surface to prevent reoxidation during soldering and help wet the surface by lowering the surface tension.[13] In Eq. 2, the surface tensions $\gamma_{\text{s-air}}$ and $\gamma_{\text{l-air}}$ should therefore become $\gamma_{\text{s-flux}}$ and $\gamma_{\text{l-flux}}$. This flux has a greater ability to reduce the interfacial tension $\gamma_{\text{l-flux}}$ between the flux and the molten solder alloy by removing the surface oxide and enhancing the fluidity of the molten solder alloy. A smaller θ value can be attained as $\gamma_{\text{l-flux}}$ decreases. Therefore, the contact angle is dramatically reduced, and the wettability of the Sn-40Bi-2Zn-0.1Cu solder was improved.

Wetting Time, Wetting Force, and Withdrawing Force

Wetting Time

Figure 4 depicts typical wetting force–time curves; the values of wetting time are collected in Table III. It can be seen that Sn-40Bi-2Zn-0.1Cu has the shortest wetting time, followed in order by Sn-40Bi-0.1Cu, Sn-58Bi, and Sn-37Pb. Since wetting is a reactive process, chemical reaction between the substrate and the molten solder is a prerequisite for wetting to occur, so the wetting time is normally regarded as the beginning of the formation of an interfacial IMC layer.[14] It can be deduced that Cu addition promoted the local Cu concentration at the solder/Cu interface, which is dominant for nucleation and growth of Cu-Sn IMC. Thus, the wetting time reduced with Cu addition. However, the reason for the reduced wetting time with Zn is different. Because Cu has higher affinity for reaction with Zn than Sn does, formation of Cu-Zn IMC would take place of Cu-Sn IMC. The driving force of Cu-Zn IMC is much larger than that of Cu-Sn IMC,[15] thus the wetting time was reduced in the Sn-40Bi-2Zn-0.1Cu solder/Cu couple.

Wetting Force and Withdrawing Force

The measured wetting forces (F_{m}) of the solders on Cu substrate are presented in Table III and Fig. 5. Several groups of oxygen-free pure copper plates were wetted into molten solders and the wetting force calculated using the equation[16,17]

$$F_{\text{m}} = c\gamma_{\text{l-air}} \cos\theta - \rho g v, \tag{3}$$

where c, ρ, g, and v are the perimeter of the specimen, the density of the molten solder, the gravitational constant, and the immersion volume of the specimen, respectively. The equilibrium wetting force is related to the surface tension of the liquid, the contact angle, and the buoyancy force. Apparently, both Cu and Zn additions promoted the wetting force of the Sn-Bi-based solder. According to Carroll and Warwick,[18] addition of Cu causes a slight increase of the surface tension of molten Sn-Pb solder, which is similar to the results of this study.

The wetting force reaches its maximum when the contact angle becomes zero before the specimen detaches from the molten solder. The buoyancy force is zero at this point, and the above-mentioned force equation becomes

$$F_{\text{w}} = c\gamma_{\text{l-air}}. \tag{4}$$

Clearly, the withdrawing force depends on the surface tension of the molten solder in air. Based on the results in Table III, Cu addition lowered the surface tension of Sn-40Bi-0.1Cu, while the surface tension rose when Zn was added. This is consistent

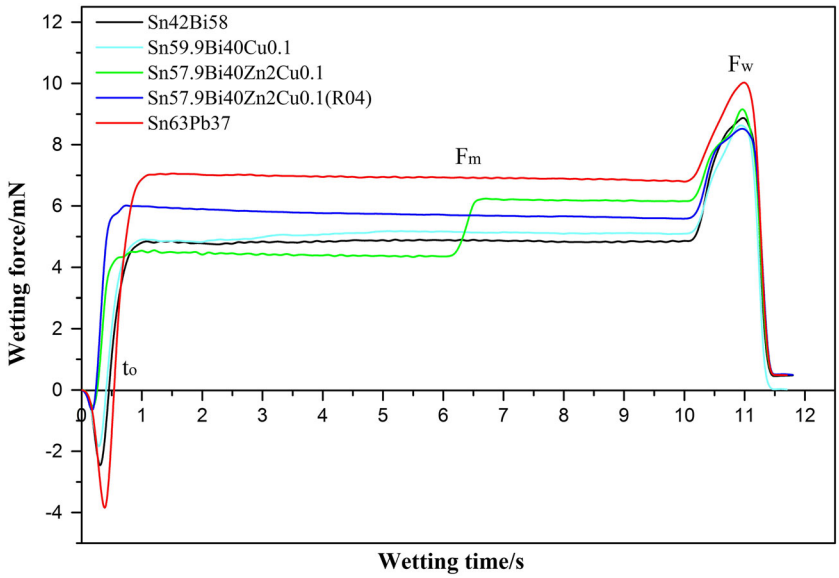

Fig. 4. Wetting balance curves of Sn-37Pb, Sn-58Bi, Sn-40Bi-0.1Cu, and Sn-40Bi-2Zn-0.1Cu solder alloys.

Table III. Average wetting times, wetting forces, and withdrawing forces of Sn-37Pb, Sn-58Bi, Sn-40Bi-0.1Cu, and Sn-40Bi-2Zn-0.1Cu solder alloys

Alloy	Average Wetting Time, t_0 (s)	Average Wetting Force, F_m (mN)	Average Withdrawing Force, F_w (mN)
Sn-37Pb	0.53 ± 0.03	6.99 ± 0.06	10.11 ± 0.06
Sn-58Bi	0.43 ± 0.06	5.10 ± 0.12	8.79 ± 0.13
Sn-40Bi-0.1Cu	0.41 ± 0.01	5.12 ± 0.07	8.61 ± 0.08
Sn-40Bi-2Zn-0.1Cu	0.32 ± 0.32	5.89 ± 0.05	9.26 ± 0.57
Sn-40Bi-2Zn-0.1Cu (adding a small amount of R04 flux)	0.29 ± 0.03	5.94 ± 0.03	8.55 ± 0.44

with the variation trend of the contact angle. Since the withdrawing force should not be affected be interfacial reactions, the nature of the elements should be taken into account. The higher surface energy of the element Zn (0.81 N/m) compared with Sn (0.55 N/m) or Bi (0.39 N/m) leads to the higher surface energy γ_{l-air} of the molten Sn-40Bi-2Zn-0.1Cu solder. This is why the average withdrawing force of the Sn-40Bi-2Zn-0.1Cu solder (9.26 mN) is higher than that for Sn-40Bi-0.1Cu solder (8.61 mN) or Sn-58Bi solder (8.79 mN).

Shear Property and Fracture Morphology

To evaluate the mechanical integrity of such solder joints, single shear joints were fabricated and tested. The detailed geometry of the solder joints used in this study is shown in Table IV. Failure occurred at the solder alloy/substrate interface when the elastic deformation ended. The shear force of the Sn-40Bi-0.1Cu solder was slightly higher than for the other two alloys. Overall, the shear force decreased in the following order: Sn-40Bi-0.1Cu, Sn-58Bi, and Sn-40Bi-2Zn-0.1Cu solder. It can be seen that Zn addition further deteriorates the shear strength of the solder joint, as it offset the improvement obtained with Cu addition. There are several reasons to explain this phenomenon: One is that a certain amount of Zn-rich phases with length of about 20 μm can be seen in Fig. 8f. Needle-like Zn particles with high aspect ratio constrained the plastic flow during tensile deformation because slip planes cannot move freely in their preferred direction, resulting in a lack of ductility. This could account for the decreased shear strength of the Sn-40Bi-2Zn-0.1Cu/Cu solder joint. Also, the shrinkage of solder during solidification and retained gases formed by volatilization of organics and reaction products lead to voids. As Zn is active and easily oxidized in the soldering process, more voids formed in the interface with the Sn-40Bi-2Zn-0.1Cu solder. During the shear fracture process, voids not only acted as a crack source but also reduced the active joint area because of stress concentration.

Table IV. Results of shear testing of Sn-Bi-based solder/Cu joints

Alloy	Fracture Position	Joint Thickness, h (mm)	Joint Diameter, d (mm)	Shear Strength, σ_c (MPa)
Sn-58Bi	Solder/Cu substrate	0.218 ± 0.019	5.008 ± 0.078	35.208 ± 1.245
Sn-40Bi-0.1Cu	Solder/Cu substrate	0.216 ± 0.020	5.132 ± 0.069	39.320 ± 1.019
Sn-40Bi-2Zn-0.1Cu	Solder/Cu substrate	0.216 ± 0.011	5.192 ± 0.041	32.177 ± 1.247

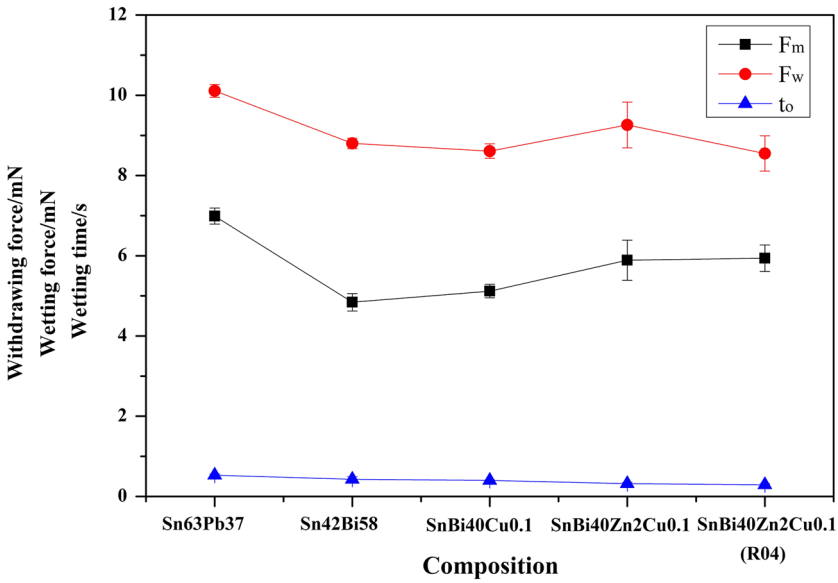

Fig. 5. Variation of wetting time, wetting force, and withdrawing force for different alloys.

Figure 6 shows SEM images of the Sn-58Bi, Sn-40Bi-0.1Cu, and Sn-40Bi-2Zn-0.1Cu solder shear joints. The microstructure of the Sn-40Bi-0.1Cu and Sn-40Bi-2Zn-0.1Cu joints consists of dendritic β-Sn and eutectic area with refined Bi-rich phase finely dispersed in the β-Sn matrix. While a coarsening Bi-rich phase with bulk morphology was found in the Sn-58Bi solder, the ductility (both elongation and percentage reduction of area) decreased and the joint became brittle. From Fig. 6c, the surface morphology and thickness of the IMC in Sn-40Bi-2Zn-0.1Cu are different from the other solders. Only granular Cu_5Zn_8 compounds existed in Sn-40Bi-2Zn-0.1Cu, while a spherical Cu_6Sn_5 layer was detected in the Sn-40Bi-0.1Cu/Cu and Sn-58Bi/Cu solder interfaces. The compositions of the IMCs on the surface as determined by EDS analysis are presented in Fig. 7. Wang et al.[15] reported that the first IMC formed during the wetting reaction would be Cu-Zn-γ phase when the Zn content is beyond 0.88%, which is consistent with this study. For the other two solders, according to Hu,[19] it is possible for two types of IMC (Cu_6Sn_5 and Cu_3Sn) to be formed between the Sn alloy and Cu substrate at the temperature of 573 K. In this work, a Cu_6Sn_5 layer was observed instead of Cu_3Sn because Cu_6Sn_5 grows much faster than Cu_3Sn in the molten state. The formation of these IMCs may be attributed to saturation of the molten solder in contact with the Cu. As reported, as the connection between the solder and substrate, the strength of Cu-Zn IMC is weaker than Sn-Cu IMC because of its brittle nature, which weakens the shear strength of Zn-containing solder.

For deeper understanding of the failure behaviors causing the strength effect in the Sn-58Bi, Sn-40Bi-0.1Cu, and Sn-40Bi-2Zn-0.1Cu solder joints, fracture surfaces after shear tests were analyzed by SEM and the results are presented in Fig. 8. Brittle fracture with a flat surface was observed on the substrate. This suggests that catastrophic fracture of the solder joint occurred, very possibly with rapid crack propagation along the thick IMC layer and a large number of pores.[20] In this study, based on the macroscopically observed fracture, the failure mode for the three solders was found to be interface-related failure, namely fracture occurred outside the bulk solder, at the Sn-rich layer/Cu interface. This indicates that the solder alloy at the bottom of the solder was torn during the shear test. Generally, if the stress is lower than the solder strength while the interfacial stress is higher

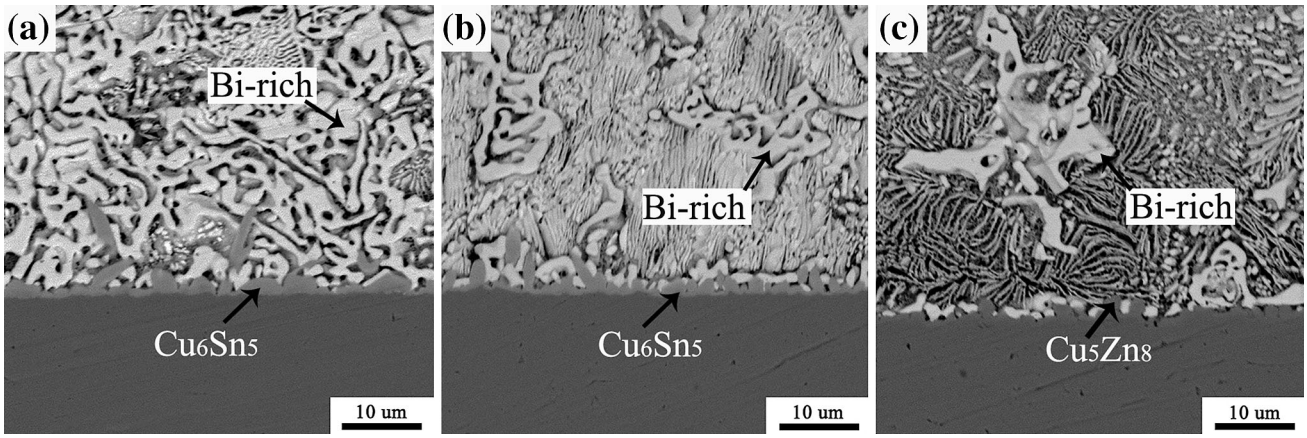

Fig. 6. SEM micrographs of interfacial microstructures of Sn-Bi/Cu solder joints: (a) Sn-58Bi/Cu, (b) Sn-40Bi-0.1Cu/Cu, and (c) Sn-40Bi-2Zn-0.1Cu/Cu.

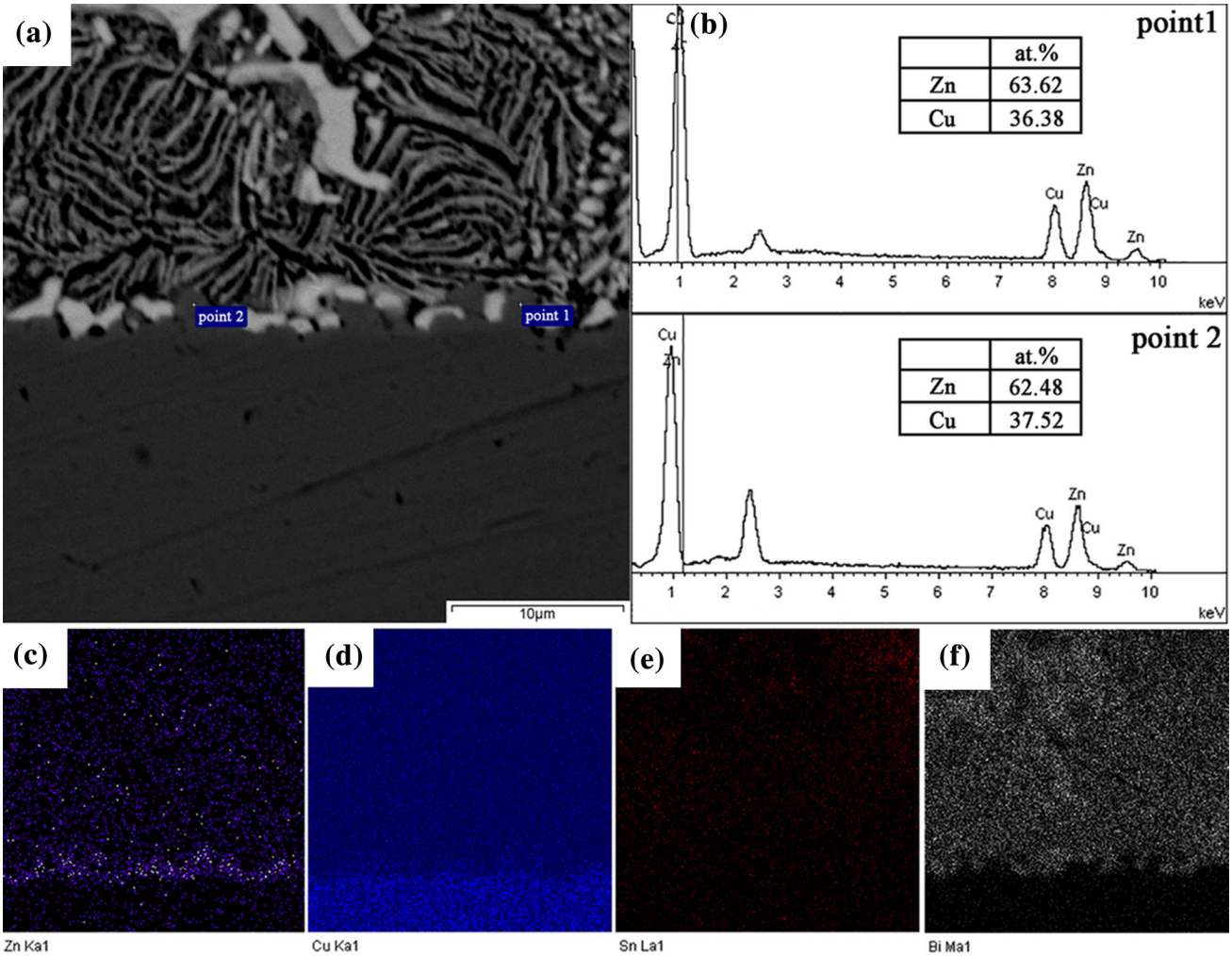

Fig. 7. EDS analysis results of the Sn-40Bi-2Zn-0.1Cu/Cu interface area: (a) microstructure, (b) chemical composition of the intermetallic compound, and map scanning results of (c) Zn, (d) Cu, (e) Sn, and (f) Bi.

than the interfacial bonding strength, the solder joint fails through the interface.[21] According to microstructural analysis, the different coefficient of thermal expansion between the solder and IMC layer/Cu substrate caused different volume stresses, which gradually evolved into residual stress. This led to failure of the solder/Cu substrate under the shear condition.

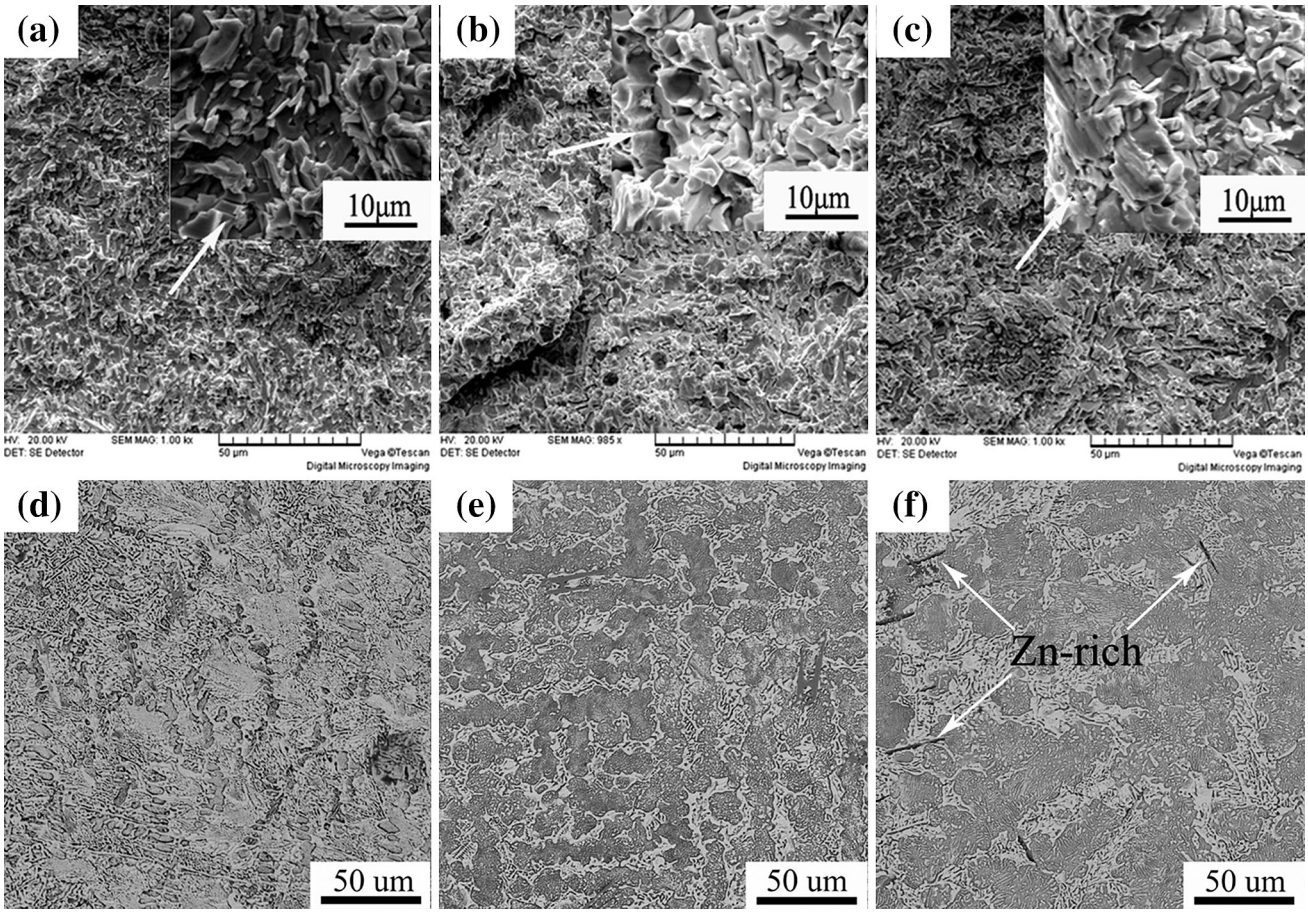

Fig. 8. Microscopic fracture structures of Sn-Bi-based/Cu solder joints: (a) Sn-58Bi/Cu, (b) Sn-40Bi-0.1Cu/Cu, and (c) Sn-40Bi-2Zn-0.1Cu/Cu, and corresponding microstructures of three solder alloys: (d) Sn-58Bi, (e) Sn-40Bi-0.1Cu, and (f) Sn-40Bi-2Zn-0.1Cu.

CONCLUSIONS

Three types of solder alloy (Sn-58Bi, Sn-40Bi-0.1Cu, and Sn-40Bi-2Zn-0.1Cu) were adopted to investigate the influence of minor Cu and Zn additions on the wettability and shear strength of Sn-Bi-based/Cu solder joints. The following conclusions can be drawn:

1. Cu addition is good for the wetting ratio of the solder alloys, while Zn was disadvantageous. The reduction of the wetting time can be ascribed to the change of the Cu concentration and the formation of Cu_5Zn_8. The wetting force increased with addition of Cu and Zn, because these two dissolved elements improved the surface energy between the solder and Cu substrate, especially for Zn. The withdrawing force changed consistently with the wetting ratio and the contact angle. Use of R04-type flux dramatically improved the wettability for the Sn-40Bi-2Zn-0.1Cu solder.
2. The shear force decreased in the following order: Sn-40Bi-0.1Cu, Sn-58Bi, and Sn-40Bi-2Zn-0.1Cu solder. Cu addition refined the grains of the Bi-rich phase and decreased the joint brittleness, which is the reason for the improved shear performance of the Sn-40Bi-0.1Cu solder. However, despite making the same contribution to refining, Zn weakened the shear strength of the solder because of its natural brittleness and chemical activity.

ACKNOWLEDGEMENTS

The projects are financially supported by the Natural Science Foundation of China (Grant No. 51375511) and Fundamental Research Funds for the Central Universities of China (Grant Nos. CDJZR12138801 and CDJZE13130033).

REFERENCES

1. T. Laruila, V. Vuorinen, and J.K. Kivilahti, *Mater. Sci. Eng. R* 49, 1 (2005).
2. Y.X. Goh, S.F. Lee, and A.S.Md.A. Haseeb, *J. Mater. Sci.* 24, 2052 (2013).
3. G.F. Ma, N. Liu, and H.F. Zhang, *J. Alloys Compd.* 456, 379 (2008).
4. J.F. Li, S.H. Mannan, M.P. Clode, and D.C. Whalley, *Acta Mater.* 54, 2907 (2006).
5. A.F. Abd El-Rehim, *J. Alloys Compd.* 440, 127 (2007).
6. J.M. Song, T.S. Lui, and Y.L. Chang, *J. Alloys Compd.* 403, 191 (2005).

7. L. Yang, C.C. Du, and J. Dai, *J. Mater. Sci.* 24, 4180 (2014).
8. S.H. Zhang and Q.F. Chen, *Compos. B Eng.* 58, 275 (2014).
9. S.K. Das, A. Sharif, Y.C. Chan, and N.B. Wong, *J. Alloys Compd.* 481, 167 (2009).
10. J.Y. Park, J.S. Ha, and C.S. Kang, *J. Mater. Res.* 29, 1146 (2000).
11. D.Q. Yu, H.P. Xie, and L. Wang, *J. Alloys Compd.* 385, 119 (2004).
12. M.J. Rizvi, Y.C. Chan, and C. Bailey, *J. Electron. Mater.* 34, 1115 (2005).
13. C.L. Chung, K.S. Moon, and C.P. Wong, *J. Electron. Mater.* 34, 994 (2005).
14. K. Zeng and K.N. Tu, *Mater. Sci. Eng. R* 38, 55 (2002).
15. H.Q. Wang, F.J. Wang, F. Gao, X. Ma, and Y.Y. Qian, *J. Alloys Compd.* 433, 302 (2007).
16. J.I. Lee, S.W. Chen, and H.Y. Chang, *J. Electron. Mater.* 32, 117 (2003).
17. H.Y. Chang, S.W. Chen, D.S. Wong, and H.F. Hsu, *J. Mater. Res.* 18, 1420 (2003).
18. M.A. Carroll and M.E. Warwick, *Mater. Sci. Technol.* 3, 1040 (1987).
19. C.J. Hang, Y.H. Tian, and R. Zhang, *J. Mater. Sci.* 24, 3905 (2013).
20. H.T. Lee, S.Y. Hu, T.F. Hong, and Y.F. Chen, *J. Electron. Mater.* 37, 867 (2008).
21. M. Sona and K. Narayan Prabhu, *J. Mater. Sci.* 25, 1446 (2014).